Envelope Analysis of Intense Laser Pulse Self-Modulation in Plasmas

Eric Esarey, Jonathan Krall, and Phillip Sprangle
Beam Physics Branch, Plasma Physics Division, Naval Research Laboratory, Washington, D.C. 20375-5346
(Received 24 September 1993)

An envelope equation describing laser pulse self-focusing and optical guiding in plasmas is derived and is used to analyze self-modulation. Included is the plasma wave generated by the pulse front, which leads to periodic focusing, radial energy transport, and laser envelope modulation. The onset criterion and growth rates are calculated and compared to simulations using the envelope equation and a nonlinear fluid code. For a long square pulse, onset of strong self-modulation occurs at one-half the power needed for optical guiding.

PACS numbers: 52.40.Nk

The propagation and guiding of intense laser pulses in plasmas is a problem of recent interest with numerous potential applications ranging from wake field acceleration to short wavelength radiation generation [1]. Optical guiding is necessary in order to propagate a laser pulse over distances larger than the vacuum diffraction (Rayleigh) length, $Z_R = \pi r_0^2/\lambda_0$, where r_0 is the laser spot size at focus and λ_0 is the laser wavelength. Possible methods for guiding laser pulses in plasmas include relativistic guiding [2-4], which requires a laser power P greater than a critical power P_c, and channel guiding [5-9], which requires a preformed plasma density channel with a depth Δn greater than a critical depth Δn_c. Recently, it has been observed via simulation that a relativistically guided pulse can undergo severe self-modulation [9-12], whereby the pulse rapidly (within a few Z_R) breaks up into an axial beamlet structure with a period equal to the plasma wavelength λ_p. Consequently, this beamlet structure can resonantly drive a large amplitude plasma wave with an axial electric field $\gtrsim 100$ GV/m [11,12]. Simulations indicate that self-modulation can occur when $P > P_c$ and $L > \lambda_p$, where L is the laser pulse length [11].

In the following, an envelope equation is derived which describes the two-dimensional (2D) evolution of laser pulses in plasmas, including the effects of relativistic and channel guiding, plasma wave generation, diffractive beam head erosion, etc. This envelope equation approach is advantageous (i) because of its simple form, which aids in physical interpretation, (ii) because of its ease in numerical solution, and (iii) because it lends itself to analytical calculations of various phenomena, such as the dispersion relation describing laser pulse self-modulation. The envelope equation is derived from the relativistic Maxwell-fluid equations, assumes that the laser pulse radial profile is approximately Gaussian, and is valid provided $a_0^2 \ll 1$ and $k_p r_0^2 \gg 1$, where $k_p = 2\pi/\lambda_p = \omega_p/c$, $\omega_p = (4\pi e^2 n_0/m_e)^{1/2}$ is the electron plasma frequency, and n_0 is the ambient electron density. Also, $a_0 \simeq 6 \times 10^{-10} \lambda_0 I^{1/2}$, where λ_0 is in μm and I is the laser intensity in W/cm^2, assuming circular polarization. In this Letter, this model is used to analyze self-modulation. The physical mechanism for self-modulation is delineated and the onset criterion, as well as growth rates in various regimes, are calculated. The results of the envelope equation are compared to Maxwell-fluid simulations using the nonlinear model described in Refs. [9,11,12].

For a long, axially uniform laser beam with a Gaussian radial profile, the results below indicate that guiding at a constant spot size is possible [7] when $P = P_M$, where $P_M/P_c = 1 - \Delta n/\Delta n_c$, $P_c(\text{GW}) \simeq 17\lambda_p^2/\lambda_0^2$, $\Delta n_c = 1/\pi r_e r_0^2$, $r_e = e^2/m_e c^2$, and a plasma density profile of the form $n = n_0 + \Delta n r^2/r_0^2$ has been assumed. A laser pulse with a finite rise time will generate a plasma wave with a density oscillation of the form $\delta n \sim |\delta n| \cos k_p(z - ct)$. This density wave enhances focusing in regions where $\partial\delta n/\partial r > 0$ and enhances diffraction where $\partial\delta n/\partial r < 0$. Hence, the envelope of a long pulse $L > \lambda_p$ which is at the guiding threshold $P = P_M$ will become modulated at λ_p. This modulated envelope resonantly enhances the density wave and the process proceeds in an unstable manner. Self-modulation is characterized by a radial transport of pulse energy. This is in contrast to the standard 1D forward Raman instability [11-14] in which modulation occurs due to an axial transport of energy.

The self-consistent laser-plasma interaction can be described by Maxwell's equations coupled to the cold electron fluid equations. In the limits $a^2 \ll 1$ and $k_p^2 r_0^2 \gg 1$, the Maxwell-fluid equations reduce to [9,10,13]

$$\left(\nabla_\perp^2 + \frac{2ik_0}{c}\frac{\partial}{\partial\tau}\right)\hat{\mathbf{a}} = k_p^2(\Delta\rho + \delta\rho)\hat{\mathbf{a}}\,, \tag{1a}$$

$$(\partial^2/\partial\zeta^2 + k_p^2)\delta\rho = -k_p^2|a|^2/2\,, \tag{1b}$$

where $\mathbf{a} = e\mathbf{A}_\perp/mc^2$ is the normalized vector potential of the laser field, $\mathbf{a} = \frac{1}{2}(a\mathbf{e}_x - ia^*\mathbf{e}_y) + \text{c.c.}$ (circular polarization, $\mathbf{a}\cdot\mathbf{a} = |a|^2$), $\delta\rho = \delta n/n_0 - |a|^2/2$, $\Delta\rho = n^{(0)}/n_0 - 1$, $n^{(0)}(r)$ is the initial electron density profile, $n_0 = n^{(0)}(0)$, and $\delta n = n - n^{(0)}$ is the perturbed electron density. In deriving Eqs. (1a) and (1b), the independent variables $\zeta = z - ct$ and $\tau = t$ were introduced, the quasistatic approximation [4] ($\partial/\partial\tau = 0$) was assumed in the electron fluid equation, Eq. (1b), and the slowly varying envelope approximation was assumed, i.e., $a = \hat{a}(r,\zeta,\tau)\exp(ik_0\zeta)$, where $|\partial\hat{a}/\partial\zeta|, |\partial\hat{a}/\partial c\tau| \ll |k_0\hat{a}|$ and $k_0 = 2\pi/\lambda_0$. Furthermore, $|\partial n^{(0)}/\partial r| \sim n^{(0)}/r_0$ and $\omega_p^2/\omega_0^2 \ll 1$ were assumed, where ω_0 is the laser frequency. In Eq. (1b), the term $\nabla_\perp^2|a|^2/2$ has been dropped from the right side, which is valid provided $k_p^2 r_0^2 \gg 1$. Notice that Eq. (1b) implies $\delta\rho = \int_0^\zeta d\zeta' g(\zeta'-\zeta)|a|^2(\zeta')$, where $g(\zeta)=(k_p/2)\times\sin k_p\zeta$ and $\zeta=0$ is defined to be at the pulse front; i.e., $\hat{a}(\zeta=0)=0$ (the pulse exists in the region $\zeta<0$). In the following, the effects of certain instabilities, such as large angle Raman scattering [13,15], are neglected.

An envelope equation describing the evolution of the laser pulse spot size $r_L(\zeta,\tau)$ can be derived using the source dependent expansion method [16], in which the radiation envelope $\hat{a}$ is expanded in a series of Gaussian-Laguerre modes, obtaining equations similar to Eqs. (14a) and (14b) of Ref. [16], which were there applied to the free electron laser. Assuming that $\hat{a}$ is adequately represented by the lowest order Gaussian mode, $\hat{a}=\hat{a}_0 \times\exp[-(1-i\alpha)r^2/r_L^2]$, then r_L evolves according to

$$\frac{\partial^2 r_L}{\partial\tau^2}=\frac{4c^2}{k_0^2 r_L^3}\left[1+\frac{r_L^2}{2\hat{a}_0}\int_0^\infty dx(1-x)e^{-(1+i\alpha)x/2}S(x)\right], \tag{2}$$

where $x=2r^2/r_L^2$, $\alpha=(k_0/4c)\partial r_L^2/\partial\tau$, and $S(x)$ is the source term appearing on the right side of Eq. (1a). Furthermore, $|\hat{a}_0|=a_0 r_0/r_L$, where r_0 and a_0 are independent of τ. At $\tau=0$, $r_L=r_0$ and $\partial r_L/\partial\tau=0$ are assumed for convenience. Hence, $a_0(\zeta)$ is the initial axial profile of the laser pulse. Since only the fundamental mode is retained, Eq. (2) is limited to the study of laser pulses with Gaussian radial profiles. Non-Gaussian profiles and certain transverse instabilities, such as filamentation or the laser-hose instability [17], can be examined by retaining higher order Gaussian-Laguerre modes.

Assuming an initial density profile which is parabolic, $n^{(0)}=n_0+\Delta n r^2/r_0^2$, then the envelope equation, Eq. (2), can be written in the form

$$\frac{\partial^2 R}{\partial\hat{\tau}^2}-\frac{1}{R^3}\left(1-\frac{P}{P_c}-\frac{\Delta n}{\Delta n_c}R^4\right) =4R\int_0^\zeta d\zeta'\cos k_p(\zeta'-\zeta)\frac{\partial}{\partial\zeta'}\frac{P(\zeta')/P_c}{[R^2(\zeta)+R^2(\zeta')]^2}, \tag{3}$$

where $P/P_c=k_p^2 r_0^2 a_0^2(\zeta)/16$, $R=r_L/r_0$, and $\hat{\tau}=c\tau/Z_R$. The second, third, and fourth terms on the left in Eq. (3) represent the effects of vacuum diffraction, relativistic focusing, and channel focusing, respectively, whereas the term on the right side represents the nonlinear coupling of the envelope to the plasma wave. Equation (3) correctly describes well-known laser pulse evolution, such as the inability of relativistic guiding to prevent the diffraction of short pulses $L<\lambda_p$ [4,9,13].

In the following analysis of self-modulation, an idealized axial pulse profile will be assumed consisting of a finite rise followed by a long flattop region. This simplifies analytic calculations and allows for a clear discussion of the physical mechanism. Realistic axial pulse profiles can be examined by numerical solution of either the envelope equation, Eq. (3), or the quasistatic Maxwell-fluid model, as was done in Refs. [11,12].

The evolution of a long, axially uniform laser beam can be examined using Eq. (3) in the limit where the nonlinear coupling term is neglected; i.e., the right side of Eq. (3) is set equal to zero. Matched beam propagation ($r_L=r_0=$const) requires that the power satisfy [7] $P=P_M$. When $P\neq P_M$, the equilibrium spot size oscillates according to $k_e^2 Z_R^2 R^2/2=\chi_+-\chi_-\cos k_e c\tau$, where $k_e^2=4\Delta n/\Delta n_c Z_R^2$ and $\chi_\pm=1-P/P_c\pm\Delta n/\Delta n_c$. For $k_e c\tau\ll 1$, $R^2=1+\chi_- c^2\tau^2/Z_R^2$, i.e., focusing for $\chi_-<0$ and expanding for $\chi_->0$.

The beam head generates a density wave given by $\delta\hat{n}=\int_0^\zeta d\zeta' h(\zeta'-\zeta)\partial|a|^2/\partial\zeta'$, where $h(\zeta)=\frac{1}{2}\cos k_p\zeta$ and $\delta\hat{n}=\delta n/n_0$. Hence, the envelope equation will have the initial form $\partial^2 R/\partial\hat{\tau}^2=\chi_- -2P\delta\hat{n}/a_0^2 P_c$, where $R(\tau=0)=1$. If $\delta n\sim\cos k_p\zeta$, then the density wave produces periodic regions of enhanced focusing and enhanced diffraction. The onset of strong self-modulation corresponds to $\chi_-\le 2|\delta\hat{n}|P/a_0^2 P_c$. If this is not satisfied, the envelope diffracts at all values of ζ (for $k_e c\tau\ll 1$) and modulation is reduced. For example, if $k_p^2 L_{\rm rise}^2\ll 1$, where $L_{\rm rise}$ is the rise length of a long flattop pulse, then $\delta\hat{n}=(a_0^2/2)\cos k_p\zeta$. In this limit, the onset of strong self-modulation occurs at half the power needed to optically guide an axially uniform pulse, i.e., $P=P_M/2$ (for $k_p^2 L_{\rm rise}^2\gg 1$, the onset power approaches $P=P_M$).

The stability of a matched, axially uniform laser beam can be examined by expanding about the matched beam solution ($r_L=r_0$). Letting $R=1+\delta R$ and assuming $|\delta R|\ll 1$, $\delta R=\delta\hat{R}\exp(ik_p\zeta)$ and $|\partial\delta\hat{R}/\partial\zeta|\ll|k_p\delta\hat{R}|$, the equation governing the perturbed spot size is given by

$$\left(\frac{\partial^2}{\partial\hat{\tau}^2}+\sigma\right)\delta\hat{R}=-ik_p\frac{P}{P_c}\int_0^\zeta d\zeta'\delta\hat{R}, \tag{4}$$

where $\sigma=4-5P/2P_c$.

For sufficiently early times, $\hat{\tau}\lesssim L_e$, where $L_e\sim 1/\Gamma$ is the e-folding length and Γ the growth rate of the instability, $\int d\zeta\delta\hat{R}\to\zeta\delta\hat{R}$; i.e., the coupling term is secular in ζ. This implies an unstable mode, $\delta\hat{R}\sim\exp\Gamma\hat{\tau}$, with a growth rate $\Gamma=\Gamma_1$, where $\Gamma_1=(\sqrt{\sigma^2+\nu^2}-\sigma)^{1/2}/\sqrt{2}$ and $\nu=-k_p\zeta P/P_c\ge 0$. The approximation $\int d\zeta\delta\hat{R}\simeq\zeta\delta\hat{R}$ is valid provided $\nu\hat{\tau}/4(\sigma^2+\nu^2)^{1/4}<1$.

For sufficiently late times, $\hat{\tau}>L_e$, the behavior of the instability can be found using asymptotic theory of convective instabilities [11,13]. Assuming $\delta\hat{R}\sim\exp[i(k\zeta-\delta\omega\hat{\tau})]$, Eq. (4) yields the dispersion relation $D=k(\sigma-\delta\omega^2)+k_p P/P_c$. The asymptotic behavior of a convective instability can be found by letting $\delta\omega'=\delta\omega-vk$, where $v=\zeta/\hat{\tau}$, and by setting $D(\delta\omega',k)=0$ and $\partial D(\delta\omega',k)/\partial k=0$ while holding $\delta\omega'$ constant. This gives $(\delta\omega^2-\sigma)^2=2k_p|v|\delta\omega P/P_c$. The asymptotic growth, $\delta\hat{R}\sim\exp(\Gamma\hat{\tau})$, can be solved in various limits. For example, letting $\delta\omega=\delta\omega_1\pm\sqrt{\sigma}$, where $|\delta\omega_1|\ll\sqrt{\sigma}$, implies $\Gamma=\Gamma_2$, where $\Gamma_2\hat{\tau}=(2\nu\hat{\tau}/\sqrt{\sigma})^{1/2}$. This is valid provided $\hat{\tau}\gg\nu/2\sigma^{3/2}$ (late-time asymptotic regime). In the limit

$|\delta\omega| \gg \sqrt{\sigma}$, $\Gamma = \Gamma_3$, where $\Gamma_3 \hat{\tau} = \sqrt{3}(2\nu\hat{\tau}^2)^{1/3}$. This is valid provided $\hat{\tau} \ll 3^{3/2}\nu/4\sigma^{3/2}$ (early-time asymptotic regime).

Numerical solutions of the envelope equation, Eq. (3), have been performed and compared to the above theoretical results as well as to numerical simulations using the nonlinear Maxwell-fluid code of Refs. [9,11,12]. Here, as in Ref. [9], the wave operator used in the fluid code is identical to that on the left of Eq. (1a). In this approximation the laser group velocity $v_g = c$ and the radially integrated laser power is constant at fixed ζ. The following simulations assume $\lambda_0 = 1$ μm and an initial normalized intensity which rises from $a^2 = 0$ at $\zeta = 0$ to its full value $a = a_0$ at $\zeta = -L_{\rm rise} = -5\lambda_p$ and remains constant out to $|\zeta|_{\max} = 15\lambda_p$. Initially, $r_L = r_0 = 10\lambda_p$ and $\partial R/\partial\tau = 0$. For fixed values of r_0/λ_p, $L_{\rm rise}/\lambda_p$, P/P_c, and $\Delta n/\Delta n_c$, the results of the envelope and fluid codes were independent of ω_0/ω_p (simulations were performed with $\omega_0/\omega_p = 30$–300).

First, consider a predominantly channel-guided case with $P = 0.1 P_c$ and $\Delta n = 0.9\Delta n_c$. In this case, the growth rate is small compared to c/Z_R and it is appropriate to compare the numerical results to the theoretical growth rate Γ_2. To compare with theory, the simulation points $\tau_0 = Z_R/5$ and $\zeta_0 = -L_{\rm rise}/2$ are taken as the "initial" values; i.e., the theoretical expressions were evaluated at $\zeta' = \zeta - \zeta_0$, $\tau' - \tau_0$, where ζ, τ are the simulation coordinates. Figure 1(a) shows plots of $\ln(\delta\hat{R})$ versus ζ' at fixed $c\tau' = 7.8 Z_R$ from $\Gamma_2\hat{\tau}$ (solid line), the envelope equation (crosses), and the fluid code (squares). Figure 1(b) shows corresponding plots of $\ln(\delta\hat{R})$ versus τ' at fixed $\zeta' = 11\lambda_p$. Virtually identical plots were obtained from the envelope code and the nonlinear fluid code (in the fluid code, r_L is defined as the radius containing 86.47% of the power). For the $P = 0.1 P_c$ case, excellent agreement among theory, the envelope code, and the fluid code is obtained.

Next, consider a relativistically guided case with $P = P_c$ and $\Delta n = 0$. In this case, the growth rate is significantly larger, such that comparison to the theoretical growth rates Γ_1 and Γ_3 is appropriate. Figure 2(a) shows plots of $\ln(\delta\hat{R})$ versus ζ' at fixed $c\tau' = 1.2 Z_R$ from $\Gamma_3\hat{\tau}$ (solid line), $\Gamma_1\hat{\tau}$ (dashed line), and the envelope equation (crosses). Figure 2(b) shows corresponding plots of $\ln(\delta\hat{R})$ versus τ' at fixed $\zeta' = 11\lambda_p$. The agreement between $\Gamma_1\hat{\tau}$ and the simulation is somewhat surprising in that the inequality $\nu\hat{\tau}/4(\sigma^2 + \nu^2)^{1/4} \ll 1$ is not well satisfied throughout the simulation.

For the $\Delta n = 0$ case, the fluid code exhibited a larger amount of modulation than the envelope code. The envelope equation assumes a Gaussian radial profile. In the fluid simulations, the radial profile deviated from Gauss-

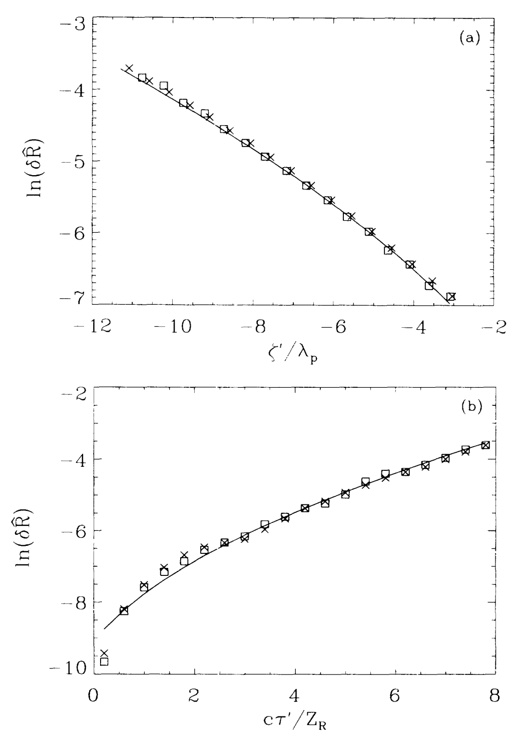

FIG. 1. Modulation amplitude $\ln(\delta\hat{R})$ plotted (a) versus ζ' at fixed $c\tau' = 7.8 Z_R$ and (b) versus τ' at fixed $\zeta' = 11\lambda_p$. Results at $P = 0.1 P_c$ are from $\Gamma_2\hat{\tau}$ (solid line), the envelope code (crosses), and the fluid code (squares).

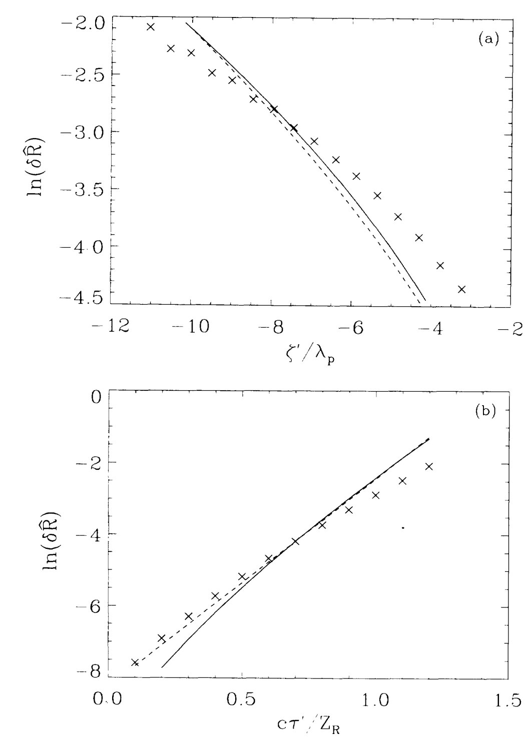

FIG. 2. Modulation amplitude $\ln(\delta\hat{R})$ plotted (a) versus ζ' at fixed $c\tau' = 1.2 Z_R$ and (b) versus τ' at fixed $\zeta' = 11\lambda_p$. Results at $P = P_c$ are from $\Gamma_3\hat{\tau}$ (solid line), $\Gamma_1\hat{\tau}$ (dashed line), and the envelope code (crosses).

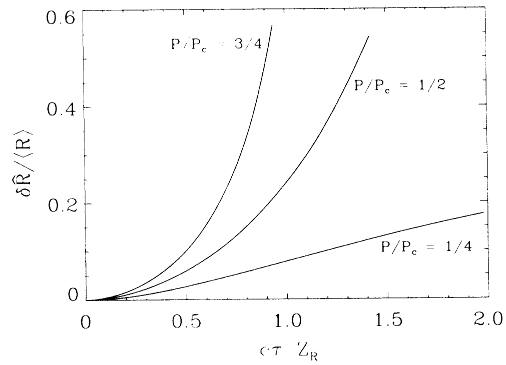

FIG. 3. Envelope code result showing the normalized modulation amplitude $\delta\hat{R}/\langle R\rangle$ plotted versus τ with $L_{\rm rise}=0.1\lambda_p$ and $P/P_c=0.25$, 0.5, and 0.75.

ian in such a way as to produce a large modulation in the intensity on axis and a relatively small modulation in the spot size; i.e., $|\hat{a}_0|=a_0r_0/r_L$ no longer holds. Simulations indicate that the degree of distortion increases as the modulation increases. In fact, for large modulation amplitude, the radial profile oscillates in ζ between a sharply peaked profile and a hollow profile.

The onset of self-modulation is illustrated in Fig. 3, which shows results from envelope code calculations with $\Delta n=0$ and $L_{\rm rise}=0.1\lambda_p$ for the powers $P/P_c=0.25$, 0.5, and 0.75. In each case, the normalized modulation amplitude $\delta\hat{R}/\langle R\rangle$ is plotted versus τ, where $\langle R\rangle$ is the ζ-averaged value of R. Theory predicts strong self-modulation to occur when $P\gtrsim P_c/2$, as is confirmed by Fig. 3. Notice that for $P/P_c=0.25$, a small degree of modulation is present even as the pulse is everywhere diffracting (R increases for all ζ).

Previous analyses of short pulse Raman scattering have assumed a 1D nonevolving, plane wave laser field [11,13,18]. These results are expected to be valid when $k_p^2r_0^2\gg 1$ and $c\tau\ll Z_R$. In the limit $c\tau\ll Z_R$, the relevant growth rates of 1D forward Raman scattering [11], $\Gamma_{\rm 1D}$, and of self-modulation, Γ_3, are related by $\Gamma_{\rm 1D}/\Gamma_3=(k_p^4r_0^2/2k_0^2)^{1/3}$. Hence, the growth of 1D forward Raman scattering becomes comparable to that of self-modulation when $k_pr_0\gtrsim\omega_0/\omega_p$. Antonsen and Mora [13] find a growth rate for small angle scattering for a 1D laser field with scaling identical to that of Γ_2; however, this is an early-time asymptotic result (Γ_2 is a late time). Although these growth rates can be comparable, such comparisons are problematic, due to the 1D versus 2D nature of the calculations. For significant propagation distances, $c\tau\gtrsim Z_R$, the 2D effects of focusing, diffraction, and guiding cannot be neglected.

Additional fluid simulations indicate that for $P\gg P_M$, self-modulation is reduced since the "effective potential" associated with the focusing forces is strong enough to overcome the diffractive effects of the plasma wave. Self-modulation may also be reduced for highly nonlinear cases in which the majority of electrons are expelled radially from the region of the laser pulse. Although severe self-modulation may be a hindrance to some applications, it can be a benefit to those requiring a large amplitude plasma wave, which is resonantly driven to large amplitudes by the modulated pulse structure.

This work was supported by the Department of Energy and the Office of Naval Research. The authors wish to acknowledge useful conversations with A. Ting and W. Mori.

[1] See, e.g., Ref. [6], and references within.
[2] A. G. Litvak, Zh. Eksp. Teor. Fiz. **57**, 629 (1969) [Sov. Phys. JETP **30**, 344 (1969)]; C. E. Max, J. Arons, and A. B. Langdon, Phys. Rev. Lett. **33**, 209 (1974); P. Sprangle, C. M. Tang, and E. Esarey, IEEE Trans. Plasma Sci. **15**, 145 (1987); W. B. Mori *et al.*, Phys. Rev. Lett. **60**, 1298 (1988).
[3] G. Z. Sun *et al.*, Phys. Fluids **30**, 526 (1987); P. Sprangle, A. Zigler, and E. Esarey, Appl. Phys. Lett. **58**, 346 (1991); A. B. Borisov *et al.*, Phys. Rev. A **45**, 5830 (1992); L. A. Abramyan *et al.*, Zh. Eksp. Teor. Fiz. **102**, 1816 (1992) [Sov. Phys. JETP **75**, 978 (1992)]; X. L. Chen and R. N. Sudan, Phys. Fluids B **5**, 1336 (1993).
[4] P. Sprangle, E. Esarey, and A. Ting, Phys. Rev. Lett. **64**, 2011 (1990); Phys. Rev. A **41**, 4463 (1990); A. Ting, E. Esarey, and P. Sprangle, Phys. Fluids B **2**, 1390 (1990).
[5] E. Esarey and A. Ting, Phys. Rev. Lett. **65**, 1961 (1990).
[6] P. Sprangle and E. Esarey, Phys. Fluids B **4**, 2241 (1992).
[7] A similar result has been derived by H. S. Brandi *et al.*, Phys. Fluids B (to be published).
[8] C. G. Durfee, III and H. M. Milchberg, Phys. Rev. Lett. **71**, 2409 (1993).
[9] P. Sprangle, E. Esarey, J. Krall, and G. Joyce, Phys. Rev. Lett. **69**, 2200 (1992).
[10] N. E. Andreev *et al.*, JETP Lett. **55**, 571 (1992).
[11] J. Krall, A. Ting, E. Esarey, and P. Sprangle, Phys. Rev. E **48**, 2157 (1993).
[12] E. Esarey, P. Sprangle, J. Krall, A. Ting, and G. Joyce, Phys. Fluids B **5**, 2690 (1993).
[13] T. M. Antonsen, Jr. and P. Mora, Phys. Rev. Lett. **69**, 2204 (1992); Phys. Fluids B **5**, 1440 (1993).
[14] J. F. Drake *et al.*, Phys. Fluids **17**, 778 (1974); C. J. McKinstrie and R. Bingham, Phys. Fluids B **4**, 2626 (1992).
[15] P. Sprangle and E. Esarey, Phys. Rev. Lett. **67**, 2021 (1991); E. Esarey and P. Sprangle, Phys. Rev. A **45**, 5872 (1992); C. B. Darrow *et al.*, Phys. Rev. Lett. **69**, 442 (1992); W. P. Leemans *et al.*, Phys. Rev. A **46**, 1091 (1992).
[16] P. Sprangle, A. Ting, and C. M. Tang, Phys. Rev. Lett. **59**, 202 (1987); Phys. Rev. A **36**, 2773 (1987).
[17] G. Shvets and J. S. Wurtele (to be published).
[18] W. B. Mori *et al.*, Phys. Rev. Lett. **72**, 1482 (1994).